

Chirality in odd- A nucleus ^{135}Nd in particle rotor modelB. Qi^a, S.Q. Zhang^{*,a,b}, J. Meng^{*,a,b,c,d}, S.Y. Wang^e, S. Frauendorff^f^a*State Key Lab Nucl. Phys. & Tech., School of Physics, Peking University, Beijing 100871, China*^b*Institute of Theoretical Physics, Chinese Academy of Science, Beijing 100080, China*^c*Center of Theoretical Nuclear Physics, National Laboratory of Heavy Ion Accelerator, Lanzhou 730000, China*^d*Department of Physics, University of Stellenbosch, Stellenbosch, South Africa*^e*Department of Space Science and Applied Physics, Shandong University at Weihai, Weihai 264209, China*^f*Physics Department, University of Notre Dame, Notre Dame, Indiana 46556, USA*

Abstract

A particle rotor model is developed which couples several valence protons and neutrons to a rigid triaxial rotor core. It is applied to investigating the chirality in odd- A nucleus ^{135}Nd with $\pi h_{11/2}^2 \otimes \nu h_{11/2}^{-1}$ configuration for the first time in a fully quantal approach. For the two chiral sister bands, the observed energies and the $B(M1)$ and $B(E2)$ values for the in-band as well as interband transitions are reproduced excellently. Root mean square values of the angular momentum components and their probability distributions are used for discussing in detail the chiral geometry of the aplanar rotation and its evolution with angular momentum. Chirality is found to change from a soft chiral vibration to nearly static chirality at spin $I = 39/2$ and back to another type of chiral vibration at higher spin.

Key words: chirality, particle rotor model, aplanar rotation, ^{135}Nd *PACS:* 21.60.Ev, 21.10.Re, 23.20.Lv

Spontaneous chiral symmetry breaking is a phenomenon of general interest in chemistry, biology and particle physics. Since the pioneering work of nuclear chirality in 1997 [1], much effort has been devoted to further explore this interesting phenomenon. Following the observation of chiral doublet

^{*}Corresponding author*Email addresses:* sqzhang@pku.edu.cn (S.Q. Zhang), mengj@pku.edu.cn (J. Meng)

bands in $N = 75$ isotones [2], more candidates have been reported over more than 20 nuclei experimentally in $A \sim 100, 130$ and 190 mass regions including odd-odd, odd- A and even-even nuclei [3, 4, 5, 6, 7, 8, 9, 10, 11, 12, 13, 14].

Chiral symmetry breaking was initially suggested to occur in a stable triaxial deformed nucleus, with a high- j particle-like valence proton (neutron) and a high- j hole-like valence neutron (proton) [1]. In this case, the angular momenta of the core, the valence proton and neutron are mutually perpendicular, arranging in the body-fixed frame into two systems with opposite chirality (left- and right-handed). Due to the restoration of chiral symmetry by quantum tunneling, a pair of near degenerate $\Delta I = 1$ bands -the chiral sister or doublet bands- are observed [1, 15].

Theory wise, chiral doublet bands were first investigated in the one-particle-one-hole-rotor model (PRM) and the corresponding tilted axis cranking (TAC) approximation [1]. Later on realistic TAC approaches, as the Strutinsky shell correction method with a hybrid Woods-Saxon and Nilsson potential [16], the Skyrme Hartree-Fock model [17], as well as the relativistic mean field model [18, 19] has been developed to investigate this new phenomena. Within the TAC mean field approximation, the left-handed and right-handed solutions are exactly degenerate. It is not possible to calculate the energy difference between the bands, which is the consequence of quantum tunneling between the two solutions. Before the onset of chirality of the mean field, the precursor of the symmetry breaking occurs as a soft vibration between the right- and left-handed configurations. These chiral vibrations have been studied in the framework of the random phase approximation (RPA) based on the TAC mean field [20, 21]. However, TAC+RPA is not able to describe the smooth transition from a slow vibration to quantum tunneling between the left- and right-handed mean field solutions. Moreover, angular momentum is not a good quantum number and the electromagnetic transitions are calculated in semiclassical approximation.

The fully quantal PRM does not suffer from these deficiencies. Total angular momentum is a good quantum number. The energies and transition probabilities are treated fully quantal. In particular, it provides the energy splitting between doublet bands covering the whole range from chiral vibrations to weak tunneling between the two chiral configurations. On the other hand, the PRM is based the assumption that the rotor has a fixed deformation. This may appear as a problem, because the nuclei in which chiral doublets have been found are considered to be soft with respect to the triaxiality parameter γ . The study in the framework of an IBA core cou-

pled to a particle and a hole found a substantial coupling between the shape and angular momentum orientation degrees of freedom [22]. In contrast, the microscopic studies in the framework of TAC+RPA [20, 21] indicate that the angular momentum dynamics is almost decoupled from the shape degrees of freedom, which justifies the application of the PRM.

For odd-odd nuclei in $A \sim 100$ and 130 regions, chirality has been extensively studied with PRM with 1-particle-1-hole configuration [23, 24], or by introducing pairing to simulate the effect of many valence nucleons [6, 25, 26, 27]. Good agreement with the experimental spectra and electromagnetic transitions has been obtained by PRM for the doublet bands in odd-odd nuclei ^{126}Cs [25], ^{128}Cs [6, 28], and ^{106}Rh [27].

Apart from odd-odd nuclei, chiral doublet bands have been observed in odd- A nuclei. The first example is the chiral spectra characteristic observed in ^{135}Nd [7], which is further confirmed by the lifetime measurements [20] and suggested to be built on the configuration $\pi h_{11/2}^2 \otimes \nu h_{11/2}^{-1}$. More candidates have been reported in ^{103}Rh [12], ^{105}Rh [9, 10] as well. For even-even nuclei, a candidate was suggested for ^{136}Nd [5], however the interpretation is doubted on the basis of the recent lifetime measurement [29]. The existence of these data makes a PRM that treats more than one valence proton and one valence neutron highly desirable. A PRM with an axial or a triaxial core coupled to many-particle configurations has been developed and used for the description of magnetic bands of $^{198,199}\text{Pb}$ [30] and the wobbling excitation in ^{163}Lu [31]. However the study of chirality with such kind of model is still absent. There has been a dispute on the identification and interpretation of chiral doublet bands based on 1-particle-1-hole configuration in odd-odd nuclei [22, 28, 29, 32, 33]. The study of the doublet bands in odd- A nuclei in the framework of a rotor coupled to two particles and one hole should shed new light on the question of nuclear chirality.

In this Letter, a triaxial n -particle- n -hole PRM will be developed to treat more than one valence proton and one valence neutron and applied to the study of nuclear chirality. The energy spectra and electromagnetic transitions probabilities of the doublet bands in ^{135}Nd will be calculated and compared with the data available as well as the previous TAC+RPA results. The structure of doublet bands with 2-particle-1-hole configuration will be discussed.

The total Hamiltonian is expressed as,

$$\hat{H} = \hat{H}_{\text{coll}} + \hat{H}_{\text{intr}}, \quad (1)$$

with the collective rotor Hamiltonian H_{coll} ,

$$\hat{H}_{\text{coll}} = \sum_{k=1}^3 \frac{\hat{R}_k^2}{2\mathcal{J}_k} = \sum_{k=1}^3 \frac{(\hat{I}_k - \hat{J}_k)^2}{2\mathcal{J}_k}, \quad (2)$$

where the indices $k = 1, 2, 3$ refer to the three principal axes of the body-fixed frame, $\hat{R}_k, \hat{I}_k, \hat{J}_k$ denote the angular momentum operators for the core, the total nucleus and the valence nucleons, respectively. The moments of inertia for irrotational flow are adopted, i.e., $\mathcal{J}_k = \mathcal{J}_0 \sin^2(\gamma - 2\pi k/3)$. The intrinsic Hamiltonian for valence nucleons is

$$\hat{H}_{\text{intr}} = \sum_{\nu} \varepsilon_{p,\nu} a_{p,\nu}^{\dagger} a_{p,\nu} + \sum_{\nu'} \varepsilon_{n,\nu'} a_{n,\nu'}^{\dagger} a_{n,\nu'}, \quad (3)$$

where $\varepsilon_{p,\nu}$ and $\varepsilon_{n,\nu'}$ are the single particle energy of proton and neutron.

The single particle states are expressed as

$$a_{\nu}^{\dagger} |0\rangle = \sum_{\alpha\Omega} c_{\alpha\Omega}^{(\nu)} |\alpha, \Omega\rangle, \quad a_{\bar{\nu}}^{\dagger} |0\rangle = \sum_{\alpha\Omega} (-1)^{j-\Omega} c_{\alpha\Omega}^{(\nu)} |\alpha, -\Omega\rangle, \quad (4)$$

where Ω is the projection of the single-particle angular momentum \hat{j} along the 3-axis and is restricted to half of the values, $-j, \dots, -1/2, 1/2, 3/2, \dots, j$, due to the time-reversal degeneracy [34], and α denotes the other quantum numbers. For a system with z valence protons and n valence neutrons, the intrinsic wave function is given as

$$|\varphi\rangle = \left(\prod_{i=1}^{z_1} a_{p,\nu_i}^{\dagger} \right) \left(\prod_{i=1}^{z_2} a_{p,\bar{\nu}_i}^{\dagger} \right) \left(\prod_{i=1}^{n_1} a_{n,\nu'_i}^{\dagger} \right) \left(\prod_{i=1}^{n_2} a_{n,\bar{\nu}'_i}^{\dagger} \right) |0\rangle \quad (5)$$

with $z_1 + z_2 = z, n_1 + n_2 = n, 0 \leq z_1 \leq z, 0 \leq n_1 \leq n$.

The total wave function can be expanded into the strong coupling basis,

$$|IM\rangle = \sum_{K\varphi} c_{K\varphi} |IMK\varphi\rangle, \quad (6)$$

with

$$|IMK\varphi\rangle = \frac{1}{\sqrt{2(1 + \delta_{K0}\delta_{\varphi,\bar{\varphi}})}} (|IMK\rangle|\varphi\rangle + (-1)^{I-K} |IM - K\rangle|\bar{\varphi}\rangle), \quad (7)$$

where $|IMK\rangle$ denotes the Wigner functions $\sqrt{\frac{2I+1}{8\pi^2}}D_{MK}^I$ and φ is a shorthand notation for the configurations in Eq. (5). The basis states are symmetrized under the point group D_2 , which leads to $K - \frac{1}{2}(z_1 - z_2) - \frac{1}{2}(n_1 - n_2)$ being an even integer with $\Omega = \dots, -3/2, 1/2, 5/2, \dots$. The reduced transition probabilities $B(M1)$ and $B(E2)$ can be obtained from the wave function of PRM with the $M1$ and $E2$ operators [26].

The single particle energy for proton and neutron $\varepsilon_{p,\nu}$ and $\varepsilon_{n,\nu'}$ in Eq. (3) are provided by the triaxial deformed single- j shell Hamiltonian [1],

$$h_{\text{sp}} = \pm \frac{1}{2}C \left\{ \cos \gamma (\hat{j}_3^2 - \frac{j(j+1)}{3}) + \frac{\sin \gamma}{2\sqrt{3}} (\hat{j}_+^2 + \hat{j}_-^2) \right\}, \quad (8)$$

where the plus or minus sign refers to particle or hole, and the coefficient C is proportional to the quadrupole deformation β as in Ref. [27].

In the PRM calculations for the doublet bands in ^{135}Nd , the configuration $\pi h_{11/2}^2 \otimes \nu h_{11/2}^{-1}$ [20] is adopted. The deformation parameters $\beta = 0.235$ and $\gamma = 22.4^\circ$ for ^{135}Nd are obtained from the microscopic self-consistent triaxial relativistic mean field calculation [18]. Accordingly, C_p and C_n in Eq. (8) take values of 0.323 and -0.323 MeV [27]. The moment of inertia $\mathcal{J}_0 = 29.0$ MeV/ \hbar^2 is adjusted to the experimental energy spectra. For the electromagnetic transition, the empirical intrinsic quadrupole moment $Q_0 = (3/\sqrt{5\pi})R_0^2 Z\beta = 4.0$ eb, gyromagnetic ratios $g_R = Z/A = 0.44$, and $g_p=1.21$, $g_n=-0.21$ are adopted [25].

The calculated excitation energy spectra $E(I)$ for the doublet bands A and B in ^{135}Nd are presented in Fig. 1, together with the corresponding data [7, 20]. The experimental energy spectra are excellently reproduced by the PRM calculation. Except for the 27/2-state in band B, the calculated results agree with the data within 50 keV. In particular, the trend and amplitude for the energy splitting between two partner bands are excellently reproduced.

For comparison, the TAC+RPA results [20] are also included. The energy splitting between two sister bands is well described for $I \leq 39/2$, which is the vibrational regime, where the RPA is stable. The energy splitting disappears at $I = 41/2$, where the TAC solution attains chirality. The description of the experiment in the region $I > 39/2$ is beyond the realm of RPA based on the planar TAC solution. Being a quantum theory that is not restricted to small amplitude vibrations, PRM is able to perfectly reproduce the energy splitting for the whole observed spin region, staying within the configuration

$\pi h_{11/2}^2 \otimes \nu h_{11/2}^{-1}$ and the triaxial rotor. The analysis below shows that the motion of the angular momentum vector in fact changes from chiral vibration about the plane spanned by the long and short axes of the triaxial shape to tunneling between the left- and right-handed configurations.

The calculated in-band and interband transition probabilities $B(M1)$ (upper panel) and $B(E2)$ (lower panel) for the doublet bands in ^{135}Nd are presented in Fig. 2, together with the available data and the TAC+RPA results [20]. For $I \leq 39/2$, the observed in-band $B(M1)$ values in the two bands are almost the same and much larger than the interband ones. These features are perfectly reproduced by the PRM calculation. The TAC+RPA gives a similar result. After $I = 39/2$ the two models differ. In the case of PRM, the interband and in-band $B(M1)$ transitions become comparable due to the transition to tunneling regime, which is absent in the TAC+RPA calculations.

For $I \leq 39/2$, the observed in-band $B(E2)$ values, in particular their similarity, are well reproduced by both the PRM and TAC+RPA calculations, while the observed interband $B(E2)$ values are underestimated in both the PRM and TAC calculations. The kink at $I = 39/2$ of the in-band $B(E2)$ values of the PRM reflects the transition to tunneling regime as mentioned in the discussion of $B(M1)$. The ratio between the in-band and interband $B(E2)$ and $B(M1)$ values depends sensitively on the details of the transition from the vibrational to the tunneling regime, which may account for the deviations of the PRM calculation from experiment.

The success in reproducing the energy spectra and transition probabilities for the doublet bands A and B in ^{135}Nd suggests that the PRM calculation must correctly account for the structure of the states. To exhibit their chiral geometry [26], we calculated for the bands A and B in ^{135}Nd the expectation values of the squared angular momentum components for the total nucleus $I_k = \sqrt{\langle \hat{I}_k^2 \rangle}$, the core $R_k = \sqrt{\langle \hat{R}_k^2 \rangle}$, the valence neutron $J_{nk} = \sqrt{\langle \hat{j}_{nk}^2 \rangle}$, and the valence protons $J_{pk} = \sqrt{\langle (\hat{j}_{(p1)k} + \hat{j}_{(p2)k})^2 \rangle}$, ($k = 1, 2, 3$), which are presented in Fig. 3 and 4.

As shown in Fig. 3, for both bands A and B, the collective core angular momentum mainly aligns along the intermediate axis (i -axis), because it has the largest moment of inertia. For $\gamma = 22.4^\circ$ the ratios between the moments of inertia are $\mathcal{J}_i : \mathcal{J}_s : \mathcal{J}_l = 6.8 : 2.6 : 1.0$. The angular momentum of the $h_{11/2}$ valence neutron hole mainly aligns along the long axis (l -axis) and that of the two $h_{11/2}$ valence protons mainly along the short axis (s -axis), which

correspond to the orientation preferred by their interaction with the triaxial core [1]. To be more precise, $\mathbf{J}_n \sim 5\hbar$ along l -axis, and both $\mathbf{J}_p \sim 10\hbar$ and $\mathbf{R} \sim 6 - 12\hbar$ lie in the plane spanned by i - and s - axis, which together form the chiral geometry of aplanar rotation.

In order to show the picture more clearly and examine the evolution of the chiral rotation, the root mean square values of the angular momentum components for the nucleus, the core, the valence neutron, and protons at spin $I = 29/2, 39/2,$ and $45/2$ are illustrated in Fig. 4. The i - and s - components of \mathbf{J}_n , and the l - components of \mathbf{J}_p and \mathbf{R} , which are negligible, have been ignored for clarity. As the total angular momentum increases, \mathbf{R} increases gradually, \mathbf{J}_n remains almost unchanged, while \mathbf{J}_p moves gradually toward the i -axis. The difference between proton and neutron is due to alignment effect by the Coriolis force, which is much weaker for the single neutron hole. At spin $I = 39/2$, where the doublet bands have smallest energy difference, the orientations of \mathbf{R}, \mathbf{J}_n and \mathbf{J}_p for band A and band B are nearly identical. Hence around this spin the structure comes closest to the ideal chiral picture of a left- and a right-handed configurations with equal components \mathbf{R}, \mathbf{J}_n , and \mathbf{J}_p along the respective i -, l -, and s -axes, which weakly communicate.

Further insight into the development of chirality with increasing angular momentum provides Fig. 5, which shows the probability distributions for the projection of the total angular momentum along the l -, i - and s -axes. For the PRM state Eq. (6), the probability for the projection K of total angular momentum on quantization axis is

$$P_K = \sum_{\varphi} |c_{K\varphi}|^2. \quad (9)$$

For triaxiality parameter $\gamma = 22.4^\circ$, the l -axis is used for quantization. The distributions with respect to the other axes are obtained by placing γ into another sector, such that the shape is the same but the principal axes are exchanged. The probability distribution of the angular momentum projection on the i -axis is given by Eq. (9) and $\gamma = 97.6^\circ$; and the distribution of the projection on the s -axis is obtained with 142.4° .

For spin $I = 29/2$, near the band head, the probability distribution of two bands differ as expected for a chiral vibration. For the lower band A the maximum probability for the i -axis appears at $K_i = 0$, whereas the probability for the higher band B is zero at $K_i = 0$, having its peak at $K_i = 25/2$. These are the typical probability distributions expected for the zero phonon state (A), which has a wave function that is symmetric in the projection on

the i -axis, and the one phonon state (B), which is antisymmetric in the same degree of freedom. The probability distributions with respect to the l -axis have a peak near $K_l = 11/2$, which is generated by the $h_{11/2}$ neutron hole. The probability distributions with respect to the s -axis have a peak near $K_s = 8$, which is generated by the pair of $h_{11/2}$ protons. Hence the chiral vibration consists in an oscillation of the collective angular momentum vector \mathbf{R} through the s - l -plane. This reveals the structure of the chiral vibration calculated by means of TAC+RPA in Ref. [20].

At spin $I = 39/2$, the probability distributions for band A and B are very similar. The distributions are peaked at $K_l = 7$, $K_i = 17$, $K_s = 17$, which corresponds to a vector with an orientation close to the vector \mathbf{I} in Fig. 4. The distributions show the characteristics of static chirality. The finite values of $P(K_i = 0)$ and $P(K_s = 0)$ reflect the tunneling between the left- and right-handed configuration, which is responsible for the remaining 76 keV energy difference between the bands. The tunneling is two-dimensional: along the i - and s -axes. If it was only along the i -axis, band B should have $P(K_i = 0) = 0$, as for the chiral vibration. The well developed tunneling regime is restricted to $I = 39/2$. For higher spin, where the energy difference between the chiral partners increases, they attain vibration character again. This is reflected by the increasing differences between the probability distributions of bands A and B. In particular the fact that $P(K_s = 0)$ is finite for band A (zero phonon) and zero for band B (one phonon) shows that the motion contains a vibration of the vector \mathbf{I} through the l - i -plane. The two vibrational regimes of our quantal calculation agree with the ones found by means of the TAC+RPA calculations in Ref. [21].

In summary, we have developed a particle-rotor model, which couples a triaxial rotor with many valence protons and many valence neutrons. We used it to investigate the chirality of the configuration $\pi h_{11/2}^2 \otimes \nu h_{11/2}^{-1}$ in the odd- A nucleus ^{135}Nd . The energy spectra of the doublet bands, the reduced probabilities $B(M1)$ and $B(E2)$ for in-band as well as for the interband transitions are reproduced excellently. Remarkably, the agreement with the data, in particular the energy splitting, is considerably better than in the case of odd-odd nuclei [23], indicating that the longer angular momentum vector of the two protons leads to more pronounced chirality. The chirality is shown to be a transient phenomenon. The chiral partner bands start as a soft vibration of the angular momentum perpendicular to the plane spanned by the short and long axes, where band A is the zero- and band B the one-phonon

state. With increasing angular momentum the vibration becomes strongly anharmonic, progressively localizing in left- and right-handed configurations. Maximal chirality is reached at $I = 39/2$, where the two bands approach each other closest. At this spin they have very similar distributions of the angular momenta of the core, the valence neutron, and the valence protons in the left- and right-handed sectors, which reflect reduced left-right tunneling. With further increasing spin the two bands again develop into the zero and one-phonon states of a chiral vibration of the angular momentum about the intermediate axis. The success of the present model encourages further application for chiral rotation in other nuclei including the even-even nuclei and settling the dispute on the identification and interpretation of chiral doublet bands based on PRM with 1-particle-1-hole configuration.

Acknowledgements

This work is partly supported by Major State Basic Research Developing Program 2007CB815000, the National Natural Science Foundation of China under Grant Nos. 10875074, 10775004, 10705004, 10505002, 10435010 and 10221003 as well as by the US Department of Energy grant DE-FG02-95ER4093.

References

- [1] S. Frauendorf and J. Meng, Nucl. Phys. A 617 (1997) 131.
- [2] K. Starosta *et al.*, Phys. Rev. Lett. 86 (2001) 971.
- [3] T. Koike, K. Starosta, C. J. Chiara, D. B. Fossan, and D. R. LaFosse, Phys. Rev. C 63 (2001) 061304(R).
- [4] R. A. Bark, *et al.*, Nucl. Phys. A 691 (2001) 577.
- [5] E. Mergel *et al.*, Eur. Phys. J. A 15 (2002) 417.
- [6] T. Koike, K. Starosta, C. J. Chiara, D. B. Fossan, and D. R. LaFosse, Phys. Rev. C 67 (2003) 044319.
- [7] S. Zhu *et al.*, Phys. Rev. Lett. 91 (2003) 132501.
- [8] P. Joshi *et al.*, Phys. Lett. B 595 (2004) 135.

- [9] J. A. Alcántara-Núñez *et al.*, Phys. Rev. C 69 (2004) 024317 .
- [10] J. Timár *et al.*, Phys. Lett. B 598 (2004) 178.
- [11] C. Vaman, D. B. Fossan, T. Koike, K. Starosta, I. Y. Lee, and A. O. Macchiavelli, Phys. Rev. Lett. 92 (2004) 032501.
- [12] J. Timár, C. Vaman, K. Starosta, D. B. Fossan, T. Koike, D. Sohler, I. Y. Lee, and A. O. Macchiavelli, Phys. Rev. C 73 (2006) 011301(R).
- [13] S. Y. Wang, Y. Z. Liu, T. Komatsubara, Y. J. Ma, and Y. H. Zhang, Phys. Rev. C 74 (2006) 017302.
- [14] E. A. Lawrie *et al.*, Phys. Rev. C 78 (2008) 021305(R).
- [15] S. Frauendorf, Rev. Mod. Phys. 73 (2001) 463.
- [16] V. I. Dimitrov, S. Frauendorf, and F. Dönau, Phys. Rev. Lett. 84 (2000) 5732.
- [17] P. Olbratowski, J. Dobazewski, J. Dudek, and W. Plóciennik, Phys. Rev. Lett. 93 (2004) 052501.
- [18] J. Meng, J. Peng, S. Q. Zhang, and S.-G. Zhou, Phys. Rev. C 73 (2006) 037303.
- [19] J. Peng, J. Meng, P. Ring, and S. Q. Zhang, Phys. Rev. C 78 (2008) 024313.
- [20] S. Mukhopadhyay *et al.*, Phys. Rev. Lett. 99 (2007) 172501.
- [21] D. Almede and S. Frauendorf, arXiv:0709.0969v1 [nucl-th]
- [22] D. Tonev *et al.*, Phys. Rev. Lett. 96 (2006) 052501, Phys. Rev. C 76 (2007) 044313.
- [23] J. Peng, J. Meng, and S. Q. Zhang, Phys. Rev. C 68 (2003) 044324.
- [24] T. Koike, K. Starosta, and I. Hamamoto, Phys. Rev. Lett. 93 (2004) 172502.
- [25] S. Y. Wang, S. Q. Zhang, B. Qi, and J. Meng, Phys. Rev. C 75 (2007) 024309.

- [26] S. Q. Zhang, B. Qi, S. Y. Wang, and J. Meng, Phys. Rev. C 75 (2007) 044307.
- [27] S. Y. Wang, S. Q. Zhang, B. Qi, J. Peng, J. M. Yao, and J. Meng, Phys. Rev. C 77 (2008) 034314.
- [28] E. Grodner *et al.*, Phys. Rev. Lett. 97 (2006) 172501.
- [29] S. Mukhopadhyay *et al.* Phys. Rev. C 78 (2008) 034311.
- [30] B. G. Carlsson and I. Ragnarsson, Phys. Rev. C 74 (2006) 044317.
- [31] B. G. Carlsson, Int. Jour. Mod. Phys. E 16 (2007) 634.
- [32] C. M. Petrache, G. B. Hagemann, I. Hamamoto, and K. Starosta, Phys. Rev. Lett. 96 (2006) 112502.
- [33] P. Joshi *et al.*, Phys. Rev. Lett. 98 (2007) 102501.
- [34] S. E. Larsson, G. Leander, and I. Ragnarsson, Nucl. Phys. A 307 (1978) 189.

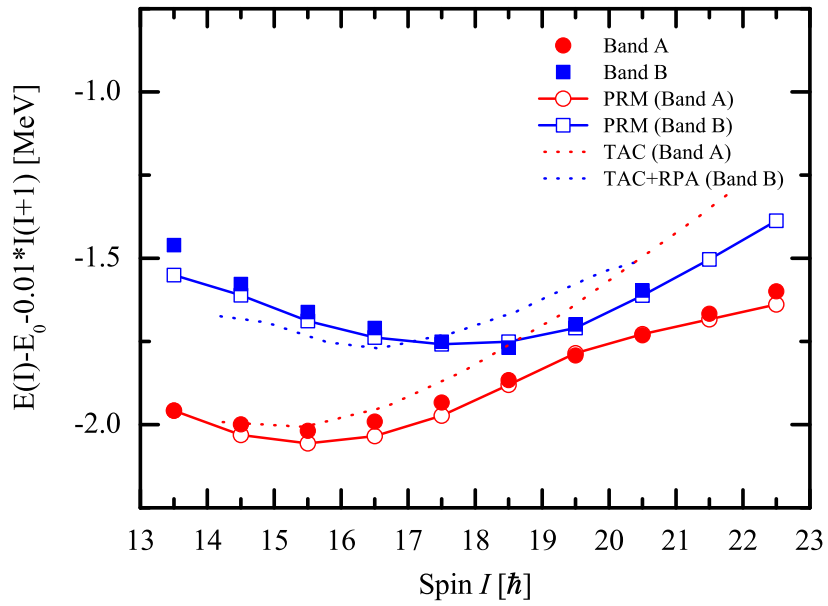


Figure 1: (color online) The excitation energies $E(I)$ for the chiral sister bands in ^{135}Nd calculated by means of the triaxial PRM with configuration $\pi h_{11/2}^2 \otimes \nu h_{11/2}^{-1}$ (open symbols) in comparison with the data (filled symbols) [7, 20] and the corresponding TAC+RPA results (dotted lines) [20]. The energies are relative to the band head E_0 of the chiral bands, with a rotor reference subtracted.

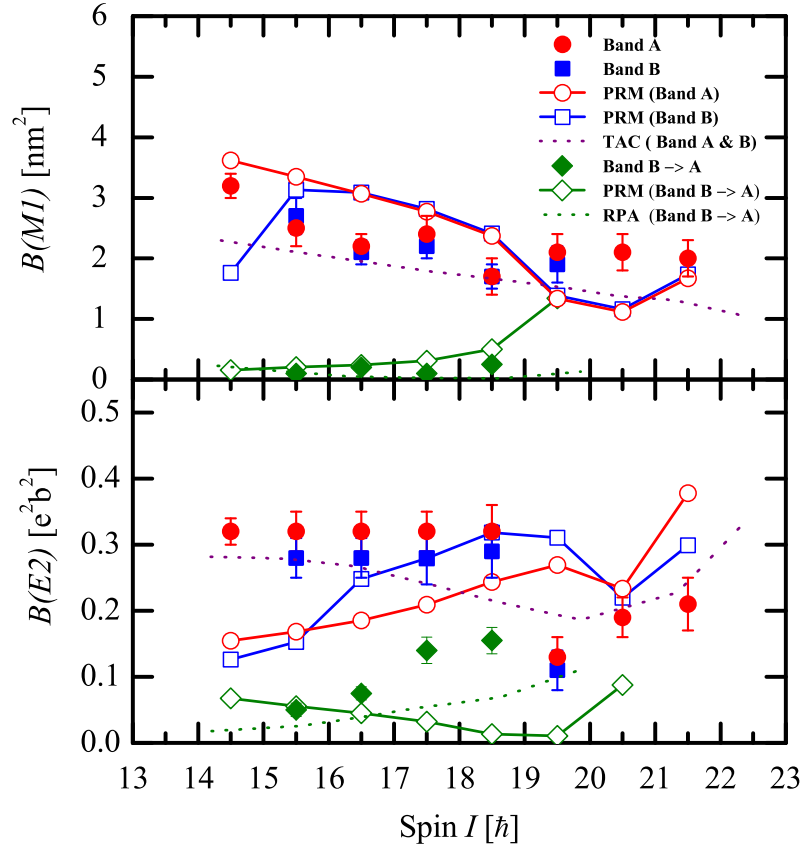


Figure 2: (color online) The $B(M1)$ and $B(E2)$ values calculated by means of the PRM for the chiral sister bands in ^{135}Nd (open symbols) in comparison with the data (filled symbols) [20] and the corresponding TAC+RPA results (dotted lines) [20].

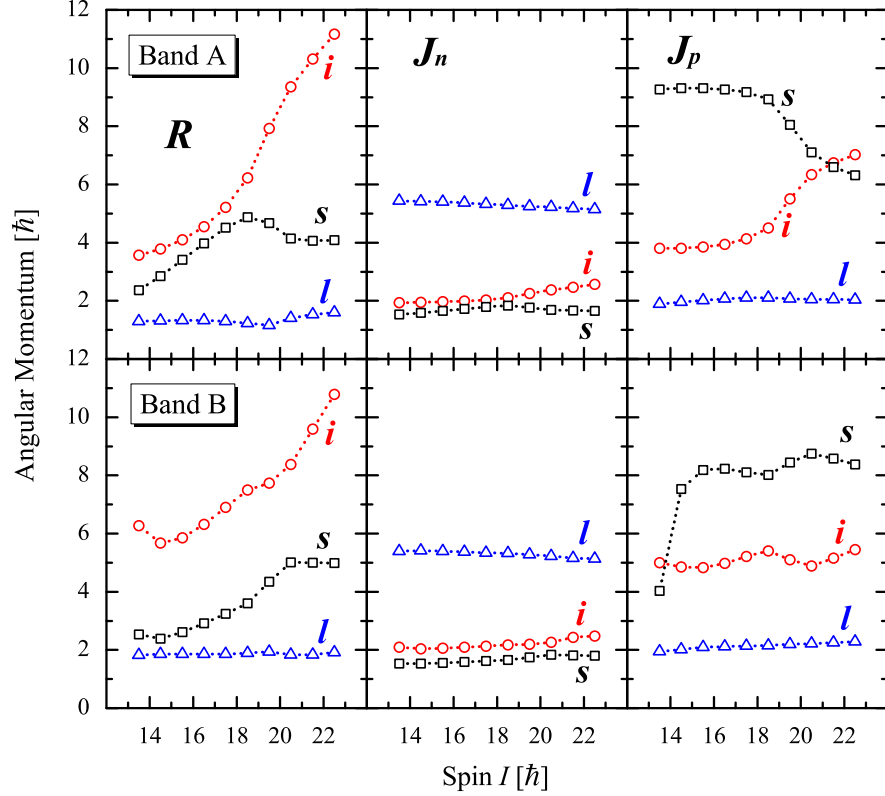


Figure 3: (color online) The root mean square components along the intermediate (i -, circles), short (s -, squares) and long (l -, triangles) axis of the core $R_k = \sqrt{\langle \hat{R}_k^2 \rangle}$, valence neutron $J_{nk} = \sqrt{\langle \hat{j}_{nk}^2 \rangle}$, and valence protons angular momenta $J_{pk} = \sqrt{\langle (\hat{j}_{(p1)k} + \hat{j}_{(p2)k})^2 \rangle}$ calculated as functions of spin I by means of the PRM for the doublet bands in ^{135}Nd .

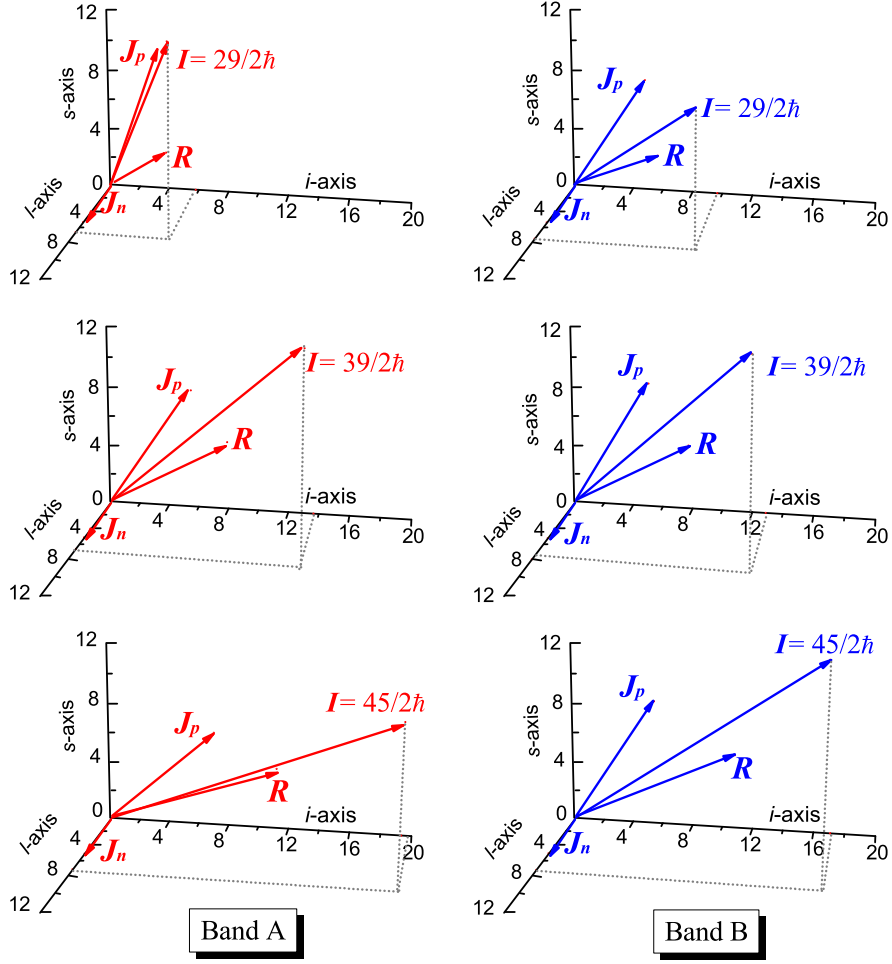


Figure 4: (color online) The angular momentum geometry in PRM for the doublet bands in ^{135}Nd at spins $I = 29/2$, $39/2$, and $45/2$.

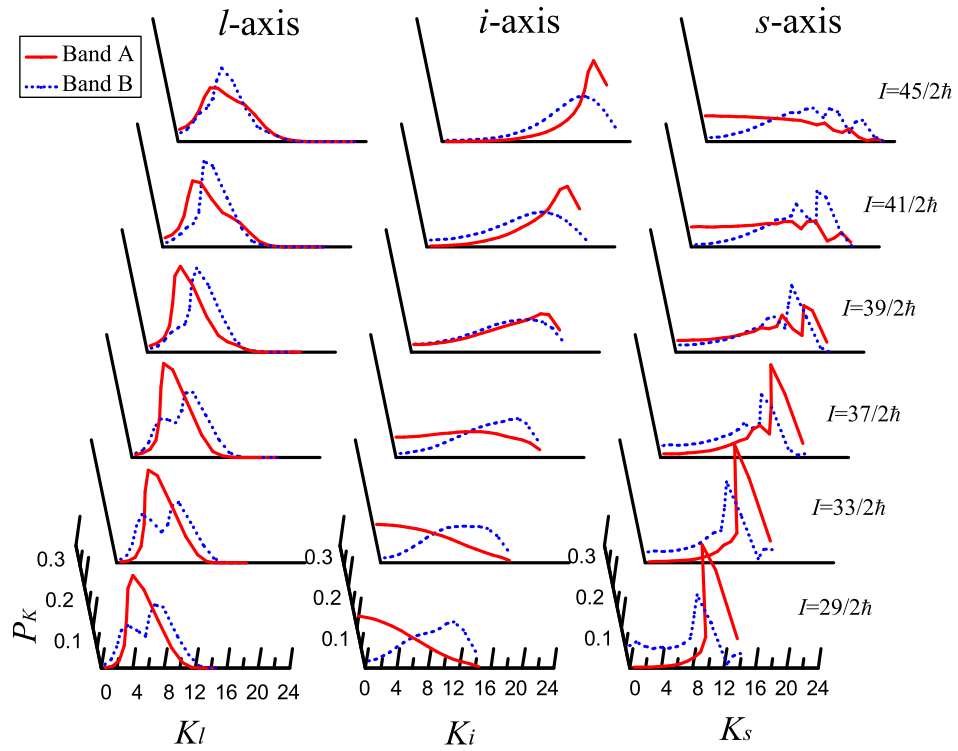


Figure 5: (color online) The probability distributions for projection of total angular momentum on the long (l -), intermediate (i -) and short (s -) axis in PRM for the doublet bands in ^{135}Nd .